

# Critical dynamics of DNA denaturation<sup>y</sup>

N. Theodorakopoulos

Theoretical and Physical Chemistry Institute,  
National Hellenic Research Foundation,  
Vasileos Constantinou 48, 116 35 Athens, Greece

M. Peyrard and T. Dauxois

Laboratoire de Physique, UMR-CNRS 5672,  
ENS Lyon, 46 Allée d'Italie,  
69364 Lyon Cedex 07, France

April 14, 2024

We present detailed molecular dynamics results for the displacement autocorrelation spectra of the Peyrard-Bishop model of thermal DNA denaturation. As the phase transition is approached, the spectra depend on whether the wavelength is smaller than, or exceeds the correlation length. In the first case, the spectra are dominated by a single peak, whose frequency approaches the bare acoustic frequency of the harmonic chain, and whose linewidth approaches zero as  $T_c - T$ . In the second case, a central peak (CP) feature is dominant, accounting for most of the weight; the linewidth of the CP appears to be temperature-independent. We also present force autocorrelation spectra which may be relevant for analyzing the statistical properties of localized modes.

## 1 Introduction

The thermal denaturation of DNA, i.e. the separation of the two strands upon heating, is a typical thermodynamic instability. It can be modelled along the lines of other thermodynamic instabilities (e.g. wetting, solid-on-solid adsorption), by associating a single, one-dimensional coordinate with the distance of a base pair[1]. Details can be found in this volume[2] and in the original literature cited there.

---

<sup>y</sup> Proceedings of the conference on \ LOCALIZATION AND ENERGY TRANSFER IN NONLINEAR SYSTEMS", June 17-21, 2002, San Lorenzo de El Escorial, Madrid, Spain. To be published by World Scientific.

<sup>y</sup>Work partially supported by EU contract HPRN-CT-1999-00163 (LOCNET network).

The equilibrium properties of the system near the phase transition are characterized by a divergent correlation length  $\xi$ , and a discontinuity in the specific heat; in other words, this is a second-order transition; the feature which sets it apart from other structural, or order-disorder transitions is that, as the transition temperature is approached from below, the order parameter diverges, i.e. the low-temperature phase becomes continuously unstable.

In this paper, we present results for the dynamical correlations of the order parameter, obtained by numerical simulation. At low and intermediate temperatures, the spectra appear to be dominated by the properties of localized anharmonic motion ("discrete breathers"). As the critical temperature is approached from below, the spectra depend solely on whether the wavelength is smaller or larger than the correlation length. In the first case, they reflect the dynamics of "islands" of the high temperature phase. In the second case, they are dominated by a strong central peak, whose width appears to depend on the wavevector, but not on the temperature.

The paper is structured as follows: Section 2 introduces the notation and numerical procedure. Section 3 presents the main results, and an analysis along the lines of relaxational/oscillational phenomenology. Section 4 is a sketch of a tentative, alternative theory, along the lines of the Mori-Zwanzig projection operator formalism. Section 5 presents a brief summary and discussion.

## 2 Notation and numerical procedure

We consider the "minimal" Hamiltonian model of homogeneous DNA denaturation proposed by Peyrard and Bishop [1] (PB),

$$H(y) = \sum_n \left[ \frac{p_n^2}{2} + \frac{1}{2R} (y_n - y_{n-1})^2 + V(y_n) \right]; \quad (1)$$

where  $y_n, p_n$  are dimensionless, canonically conjugate coordinates and momenta of the  $n$ th base pair transverse to the chain, and  $V(y) = (1 - e^{-y})^2$ .  $R$  is a dimensionless parameter which describes the relative strength of on-site vs. elastic interactions; here  $R = 10:1$ .

The thermodynamic properties of (1) have been reviewed in Ref. 2. This work describes the spectra of dynamical correlations

$$S_{AA}(q; \omega) = \frac{1}{N} \sum_{m,n} \int_{-1}^{+1} \frac{dt}{2} e^{-i\omega t} e^{iqa(n-m)} \langle A_n(t) A_m(0) \rangle \quad (2)$$

where, in this paper, mostly  $A_n = y_n$ . The integral of (2) over all frequencies,

$$S_{AA}(q) = \sum_{m,n} \int_{-1}^{+1} d\omega S_{AA}(q; \omega) = \frac{1}{N} \sum_{m,n} \langle A_n A_m \rangle \quad (3)$$

can be computed exactly using the transfer-integral result for the equilibrium correlations (cf. Eq. 55 of Ref. 2). It is expedient to consider normalized spectral functions

$$\hat{S}_{AA}(\mathbf{q};!) = \frac{S_{AA}(\mathbf{q};!)}{S_{AA}(\mathbf{q})} \quad ; \quad (4)$$

The angular brackets in Eqs. (2)–(3) denote canonical ensemble averages. Typically, we implemented this by repeated molecular dynamics (MD) simulations of the system for many different initial conditions, Fourier-transforming the spatiotemporal correlations obtained from each run, and averaging over all runs to obtain the final result.

The equations of motion,

$$\ddot{y}_n = \frac{1}{R} (\ddot{y}_{n+1} + \ddot{y}_{n-1} - 2\ddot{y}_n) - V''(y_n) \quad ; \quad n = 1; 2; \dots; N \quad (5)$$

with periodic boundary conditions,  $y_0 = y_N$ ,  $y_{N+1} = y_1$ , and typical system size  $N = 1024$ , were numerically integrated for an interval  $T = 410$ , using a 4-th order Runge-Kutta algorithm, with a time step equal to 0.02. Initial conditions were "canonical", in the sense that (i) the velocities  $\dot{y}_n$  were Gaussian-distributed, and (ii) the positions  $y_n$  were random variables distributed according to the potential energy part of the Hamiltonian (1); in addition, the system was "thermalized" for a certain time, using a Nose procedure[3].

### 3 Spectra: Phonons vs. central peak

At intermediate temperatures, the spectra are characterized by an anharmonic phonon component and a strong, low-frequency intensity (cf. Fig. 1a); this low-frequency component becomes even more pronounced at lower values of the wavevector. There is considerable residual structure in the spectrum; in particular, a secondary peak at lower frequencies appears to be a consistent feature.

As the temperature increases, and the instability approaches, the structure becomes significantly simpler. The decisive quantity is the correlation length  $\xi$ . If the wavelength is shorter than  $\xi$ , i.e.  $q = (2\pi/\lambda) > 1/\xi$ , the spectrum in effect probes the "droplets" of the high-temperature phase, of typical size  $\xi$ , which are present in the low-temperature phase; consequently, the main feature of Fig. 1b is a peak, from the acoustic phonons[3]. At the smallest values of the ratio  $q = (2\pi/\lambda)$ , a central peak (CP) feature begins to grow, and eventually dominates the spectrum at values  $q = (2\pi/\lambda) < 1/\xi$ ; this is the case in Fig. 2.

A first attempt to analyze the data can be made in terms of a phenomenological relaxation/oscillation spectral function, similar to the one

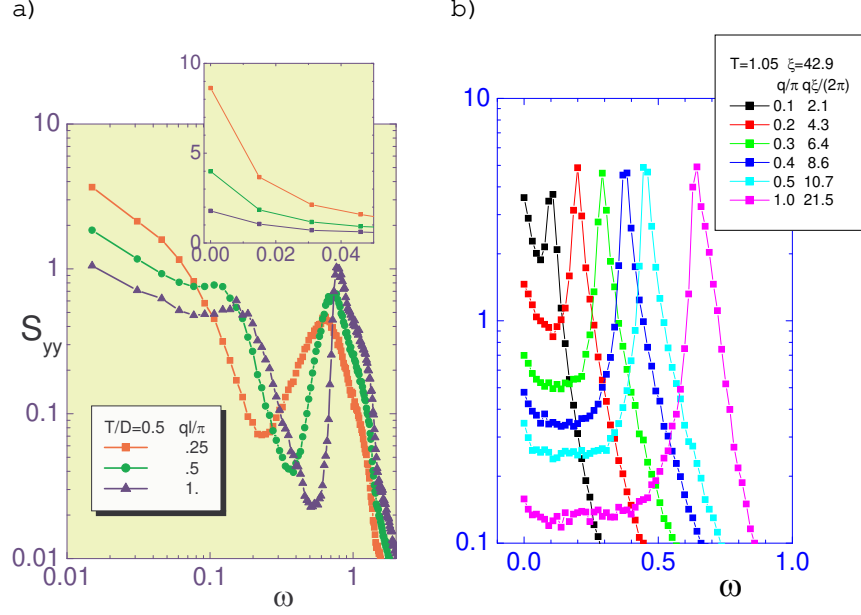


Figure 1: Normalized dynamical correlation spectra. Panel (a) presents the results at  $T = 0.5$ , for selected values of  $q$ . The inset shows the zero-frequency details (linear frequency scale). Panel (b) presents results at  $T = 1.05$ , for a variety of  $q$  values. The inset shows the ratio of the correlation length and the wavelength. If the wavelength is smaller than the correlation length, the spectrum is dominated by the phonon peak. At this length scale, the spectra probe the "droplets" of the high-temperature phase present in the system. Note the gradual buildup of a central peak at the lowest values of  $q$ .

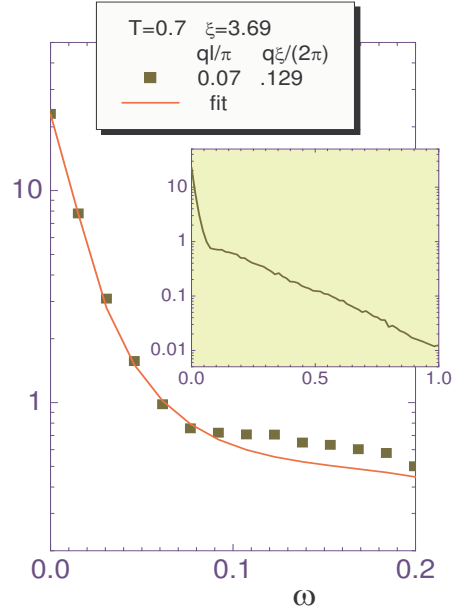


Figure 2: Normalized dynamical correlation spectra at  $T = 0.7$ , and  $q\xi/\pi = 0.07$ . At long-wavelengths (compared to  $\xi$ ) the spectrum is dominated by the CP feature. The inset shows that the tail of the spectra drops off with a different slope. The fit has been obtained using Eq. (6).

used in analyzing structural phase transitions[4], i.e.

$$\hat{S}_{yy}(q; \omega) = \frac{1}{\omega} \text{Im} \frac{\hat{\chi}_0^2}{\hat{\chi}_0^2 - \omega^2 - i\omega} \quad (6)$$

where  $\hat{\chi} = \hat{\chi}_0 + \hat{\chi}_1 \omega^2 = (\hat{\chi}_i \omega^i)$  is a relaxational memory kernel, and the  $q$ -dependence of all the parameters has been suppressed. If  $\hat{\chi}_0 \omega^2 = 0$ , it is possible for the spectrum (6) to split into phonon-like

$$\hat{S}_{yy}(q; \omega) = \frac{1}{\omega} (1 - \frac{\hat{\chi}_1^2 \omega^0}{(\hat{\chi}_1^2 \omega^2)^2 + (\hat{\chi}_0)^2}) ; \quad \omega \neq 0 \quad (7)$$

and CP

$$\hat{S}_{yy}(q; \omega) = \frac{1}{\omega} \frac{\hat{\chi}_0}{\hat{\chi}_1^2 \omega^2 + \omega^2} ; \quad \omega = 0 \quad (8)$$

contributions, where  $\hat{\chi}_1^2 = \hat{\chi}_0^2 + \hat{\chi}_1^2 \omega^2$ ,  $\hat{\chi}_1^2 = \hat{\chi}_1^2 \omega^2$ , and  $\hat{\chi}_0 = (1 - \hat{\chi}_1^2 \omega^2)$ .

Fig. 3a shows that the CP linewidth  $\hat{\chi}_0$  is largely independent of temperature; it does however depend on  $q$ , roughly linearly, as long as  $q = (2\pi/\xi)$  does not exceed unity, i.e. as long as the CP is appreciable.

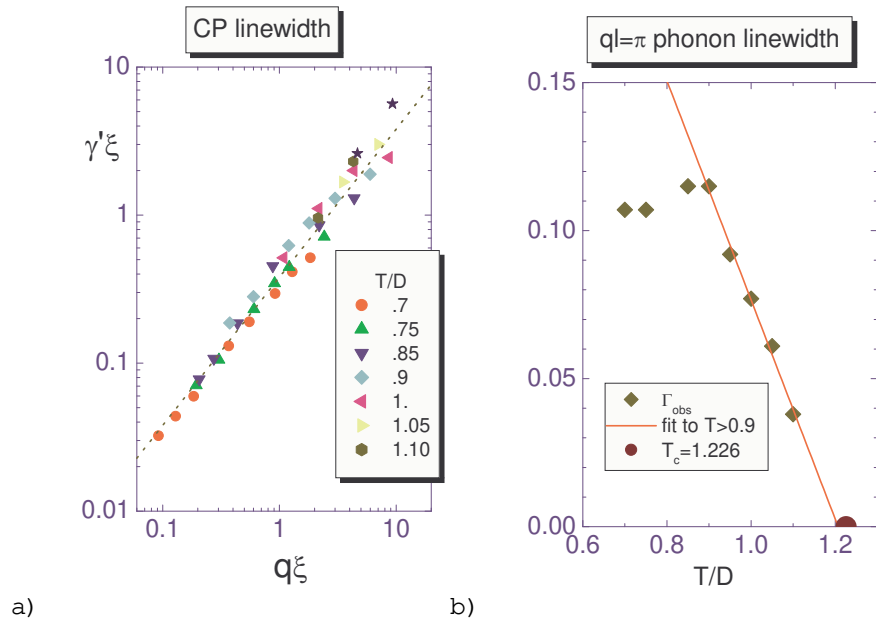


Figure 3: Line widths. Panel (a) presents the line width of the central peak as a function of wavelength. The dashed line has unit slope. Panel (b) presents the line width of the  $q = \pi$  phonon as a function of temperature. The line width extrapolates to zero at a temperature not far from  $T_c$ .

Returning to the phonon peak, it is possible to follow the decreasing phonon linewidth as the transition is approached and the dynamics – with the exception of the very long wavelengths  $q \rightarrow 0$  – evolves towards the harmonic limit (Fig. 3b). Our data is consistent with a linear critical slowing down, i.e.  $\gamma_{ph} / T_c \rightarrow T$ .

## 4 Force autocorrelations

It is instructive to consider the spectrum of the force autocorrelations, i.e.  $A_n = \langle f_n^2 \rangle = \langle V^0(y_n) \rangle$  in Eqs. (2) – (4). At low temperatures one might try to describe the spectra in terms of a crude model of independent local modes (ILM), i.e. site-independent solutions of the  $R \rightarrow 1$  (anticontinuum) limit of (5). The explicit form of the second time derivative is

$$f_n(t) = \sum_{i=1}^{N-1} \frac{\cos(\omega_i t + \phi_i)}{\omega_i^2} \quad (9)$$

where  $0 < \phi_i < \pi$ ,  $0 < \omega_i < \omega_{max}$  depend on the initial conditions and  $\omega_i^2 = 1 - 2\epsilon_i$  is the energy of the ILM. Since  $R \rightarrow 1$ , the above form should be a good approximation to exact one-site discrete breathers[6]. The canonical average of autocorrelations of (9) is

$$\langle f(t)f(0) \rangle = \frac{1}{Z} \int_0^{\omega_{max}} d\omega Q(\omega) f(t)f(0) \quad (10)$$

where  $Q(\omega) = \frac{1}{Z} \exp(-\beta \omega^2)$  and  $Z$  is determined from the normalization condition  $\int_0^{\omega_{max}} d\omega Q(\omega) = 1$ . The MD force spectra at  $T = 0.2$  are shown in Fig. 4a, along with a numerical Fourier transform of (10). Overall agreement is satisfactory, except for the very low frequency part of the spectrum.

At higher temperatures, force autocorrelation spectra exhibit the following features: (i) a very pronounced dip occurring almost exactly at the bare acoustic frequencies  $\omega_q = (2\pi/R) \sin(q/2)$ , characteristic of the high-temperature phase, and (ii) a roughly  $q$ -independent decay at higher frequencies. The observed form of the force spectra motivates an improved version of (6), with  $\omega_0^2 = T/S(q)$ , as demanded by the Mori-Zwanzig projection operator formalism [5], and  $\text{Re } \omega_c = \omega_0 \exp(-\beta \omega_c^2) + \omega_1$ , where  $\omega_1 = a(1 - \omega_q^2)^{3/2}$  if  $\omega < \omega_q$ , and  $\omega_1 = b(1 - \omega_q^2)^{1/2} \exp(-\beta \omega_c^2)$  if  $\omega > \omega_q$ . Preliminary fits obtained with this improved Ansatz for the memory function (approximating  $\text{Im } \omega$  by a constant, equal to its value at the peak, and setting  $\omega_c$  equal to the value obtained by the exponential decay constant of force spectra, cf. above and Fig. 4b) are shown in Fig. 5; they seem to reproduce the MD data much better, using the same number of adjustable parameters.

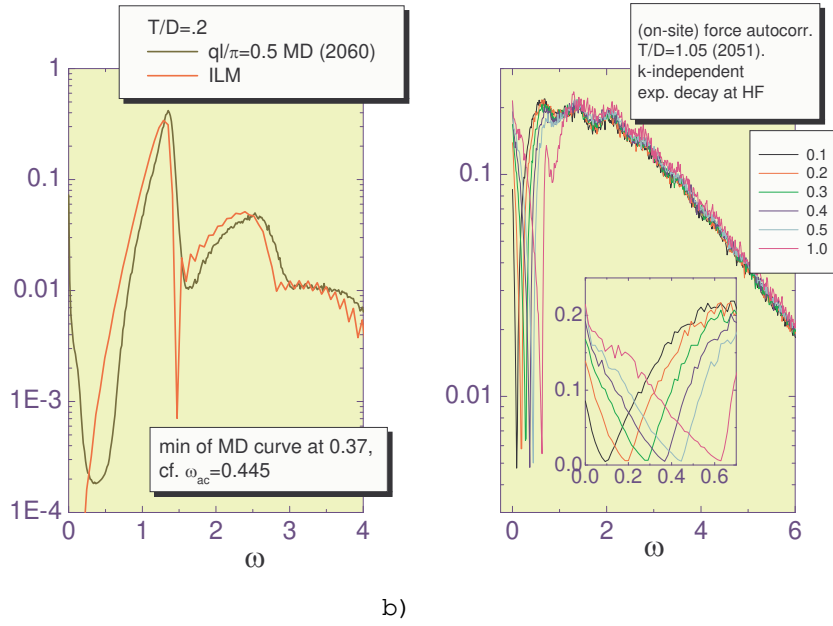


Figure 4: Normalized spectra of force autocorrelations. Panel (a) shows the results at low temperatures. The wavy curve is a theoretical estimate based on an independent localized mode picture, i.e. the normalized spectrum of (10). Panel (b) presents results at higher temperatures. Note (i) the extreme dip, almost to zero intensity, which occurs almost exactly at the acoustic phonon frequencies (inset), and (ii) the exponential decay at higher frequencies.

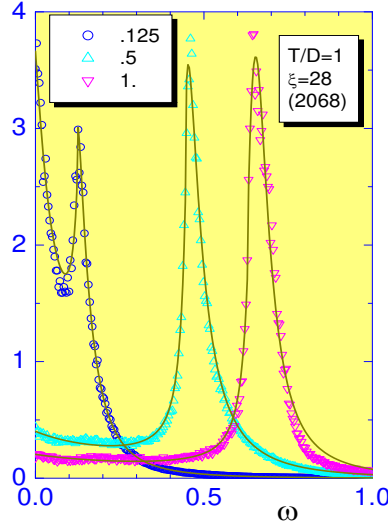


Figure 5: The spectra  $S_{yy}$  at  $T = 1.0$ . Fits are obtained with the improved Mori-Zwanzig Ansatz, which incorporates a memory kernel with a dip, similar to the one shown in Fig. 4b.

## 5 Concluding remarks

The MD data presented show that the critical dynamics of the Peyrard-Bishop model of DNA thermal denaturation can be thought of as follows: At length scales shorter than the correlation length, which correspond to "droplets" of the high temperature phase, the system reflects the properties of the unstable phase; oscillatory dynamics of the soft, acoustic phonons is the result. The linewidth of these phonons appears to vanish linearly as  $T_c - T$  ("critical slowing down"). At length scales longer than the correlation length, the dynamics is dominated by the central peak. Fluctuations are stronger, as evidenced from the divergence of the static structure factor  $S(q)$ ; the typical time scales of these fluctuations appears however to be non-critical. It remains a challenge to the theory to establish whether these "non-critical",  $q$ -dependent dynamics can be associated with localized excitations. The preliminary analysis performed at low temperatures suggests that a picture of independent localized modes provides a reasonable description of the force autocorrelations – with the important exception of the very low frequency regime. Perhaps a more detailed theory of discrete breather statistical mechanics can improve our understanding of this part of the spectra.

## References

- [1] M .Peyrard and A .R .B ishop, Phys. Rev. Lett. 62, 2755 (1989).
- [2] N .Theodorakopoulos, this volume (cond-m at/021088).
- [3] T .D auxois, M .Peyrard and A .R .B ishop, Phys. Rev. E 47, R 44 (1993).
- [4] F .Schwabl, Phys. Rev. Lett. 28, 500 (1972).
- [5] D .Forster, Hydrodynamic Fluctuations, Broken Symmetry and Correlation Functions, Benjamin, New York (1976).
- [6] J .L Marin and S .Aubry, Nonlinearity 9, 1501 (1996).